

# PHYSICAL REVIEW LETTERS

VOLUME 31

15 OCTOBER 1973

NUMBER 16

## Vibrational Excitation of $O_2$ by Electron Impact above 4 eV\*

S. F. Wong, M. J. W. Boness, and G. J. Schulz

*Department of Engineering and Applied Science, Mason Laboratory, Yale University,  
New Haven, Connecticut 06520*

(Received 20 August 1973)

Vibrational excitation of  $O_2$  by electrons in the energy range 4–15 eV is studied with a crossed-beam double electrostatic analyzer. The differential vibrational cross sections for  $v=1-4$  at  $25^\circ$  show a bell-shaped energy dependence peaked near 9.5 eV. The observations are interpreted in terms of resonant contributions by excited states of  $O_2^-$ . There is also evidence for the resonant enhancement of electronic excitations.

Direct vibrational excitation of homonuclear diatomic molecules by electron impact is, in general, an inefficient process because of the small electron-to-molecule mass ratio, as well as the lack of electric dipole moment for interaction. However, it has been well established<sup>1</sup> that in the energy range in which the incident electron can attach to form a temporary negative ion, vibrational excitation cross sections can be enhanced by orders of magnitude. Since electron attachment is essentially a vertical transition process, valuable information on the negative-ion states in the Franck-Condon region of the molecule can be inferred.

Molecular oxygen provides an important and interesting system for electron impact studies. The lowest electron configuration of  $O_2$  possesses only two electrons in its highest unfilled  $2p\pi_g$  orbital.<sup>2</sup> This gives rise to a triplet  $X^3\Sigma_g^-$  ground state and two low-lying excited singlet states,  $a^1\Delta_g$  (0.977 eV) and  $b^1\Sigma_g^+$  (1.627 eV). The lowest shape resonance is formed by adding a  $2p\pi_g$  electron to the  $X^3\Sigma_g^-$  ground state,<sup>3</sup> and its decay gives rise to vibrational excitation in the energy range 0–1.6 eV. Because this resonance is long lived, the energy dependence of the vibrational cross section in this energy range consists of a series of spikes.<sup>3</sup> We report in this

paper the observation of another large vibrational excitation region, which covers the energy range from 4 to 15 eV. In this energy range, *excited states* of  $O_2^-$  are responsible for the enhancement of the vibrational cross section. In particular, we postulate that the resonance which is predominant in this energy range consists of the  $X^3\Sigma_g^-$  ground state plus a  $2p\sigma_u$  electron, forming a  $^4\Sigma_u^-$  state of  $O_2^-$ . This appears to be the first time that a second shape resonance connected with the ground electronic state has been shown experimentally to contribute a large vibrational excitation.

The crossed-beam apparatus adopted in the present study has been described previously.<sup>4</sup> Therefore, only a brief discussion is given. An electron gun and a cylindrical electrostatic monochromator are used to form a monoenergetic electron beam. This beam is then accelerated with electron lenses to the required energy and crossed with the  $O_2$  beam at right angles in the collision region, which is shielded from stray electric or magnetic fields. Electrons scattered into the acceptance angle of another similarly constructed cylindrical electrostatic analyzer are energy selected. The transmitted electrons are detected with a Bendix helical Channeltron. Signal pulses from the Channeltron are amplified,

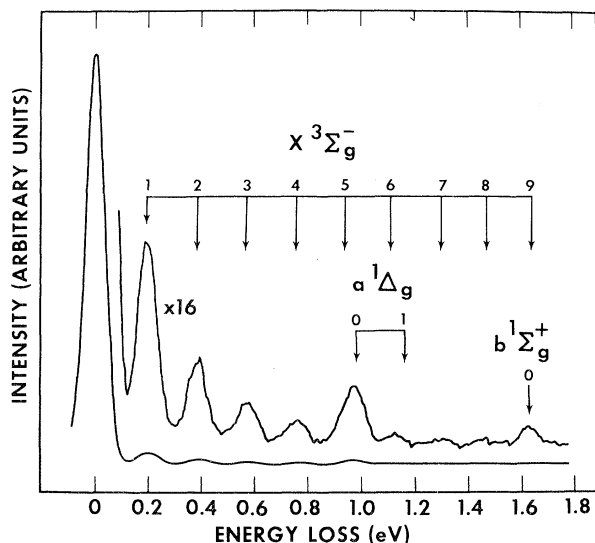


FIG. 1. Energy-loss spectrum of  $O_2$  at an incident energy of 8.28 eV and a scattering angle of  $25^\circ$ . The energies of the vibrational levels of the  $X^3\Sigma_g^-$ ,  $a^1\Delta_g$ , and  $b^1\Sigma_g^+$  states are indicated by arrows.

discriminated against noise, and finally accumulated on a signal averager.

In the present experiment, the scattering angle  $\theta$  is fixed at  $25^\circ$ . The apparatus resolution (full width at half-maximum) is set to about 60 meV, as determined from the profile of the 11.48-eV resonance in  $N_2$ .<sup>5</sup> The energy scale is calibrated against the 19.34-eV resonance in helium<sup>6</sup> by admixing a small amount of helium into the oxygen molecular beam.

Absolute differential cross sections for vibrational or electronic excitations of  $O_2$  are determined by a procedure previously used.<sup>4</sup> They are obtained as a product of two independent measurements, namely, the ratios of inelastic to elastic differential cross section,  $\sigma_v/\sigma_e$ , and the elastic cross section alone. The ratios  $\sigma_v/\sigma_e$  for a given electron energy are readily obtained from the corresponding peak heights derived from the energy-loss spectrum. The elastic cross section in  $O_2$  is obtained by comparing the elastically scattered current in  $O_2$  with the elastically scattered current in helium at the same pressure. The differential cross section in helium is known from the theoretical work of LaBahn and Callaway.<sup>7</sup> Thus we refer the elastic cross section in  $O_2$  to their theory. Figure 1 shows an example of the energy-loss spectrum obtained at an incident electron energy of 8.28 eV. The experimental errors of the differential cross sections

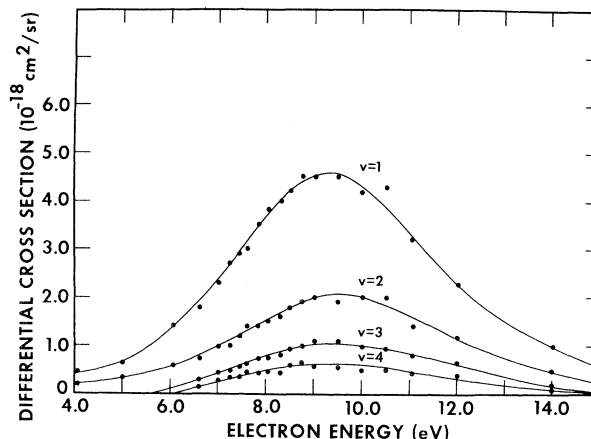


FIG. 2. Energy dependence of the differential vibrational cross sections for  $v=1-4$  of  $X^3\Sigma_g^-$ . The experimental errors in the cross sections are about 30%.

reported in this paper are estimated to be on the order of 30%. In fact, our measured differential elastic cross section in the energy range 4–15 eV is in good agreement with the results of Trajmar, Cartwright, and Williams.<sup>8</sup>

The energy dependence of the differential vibrational cross section at  $25^\circ$  for  $v=1-4$  of the  $X^3\Sigma_g^-$  ground state are shown in Fig. 2. All curves show a bell-shaped structure with a broad peak near 9.5 eV. While smooth curves are drawn to pass through the experimental data, the possibility of fine structures<sup>9</sup> comparable in width to the separation of the data points and of similar magnitude to the noise level of the present data is not excluded.

From Fig. 2 the maximum differential vibrational cross section for  $v=1$  is approximately  $4.6 \times 10^{-18} \text{ cm}^2/\text{sr}$ . The maximum vibrational cross sections for  $v=2, 3, 4$  are, successively, reduced approximately by a factor of 2.

The energy dependence of the differential electronic cross sections for the metastable states  $a^1\Delta_g$  and  $b^1\Sigma_g^+$  at  $25^\circ$  is shown in Fig. 3. Our data show a broad peak for the differential cross section of the  $a^1\Delta_g$  and  $b^1\Sigma_g^+$  states near 8.0 and 9.0 eV, respectively. The experimental results obtained by Trajmar, Cartwright, and Williams<sup>8</sup> at  $20^\circ$  are shown by open triangles for comparison. Both results agree within their error limits.

From Fig. 3 the maximum differential electronic cross section for the  $a^1\Delta_g$  state at  $25^\circ$  near 8.0 eV is  $(1.2 \pm 0.4) \times 10^{-18} \text{ cm}^2/\text{sr}$ , about 2 orders of magnitude larger than that calculated by Julienne and Krauss,<sup>10</sup> using an Ochkur-Rudge approxima-

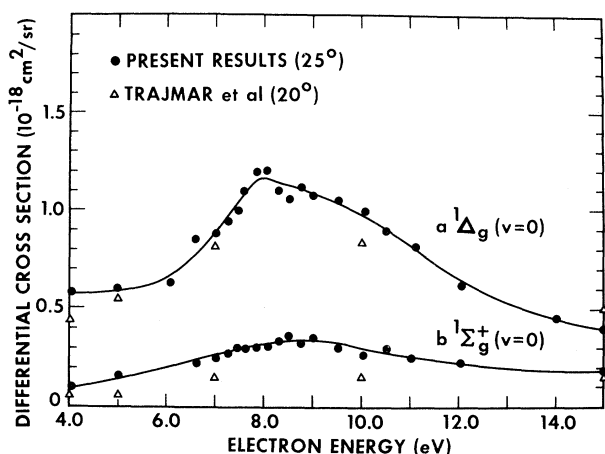


FIG. 3. Energy dependence of the differential electronic cross sections for the states  $a^1\Delta_g$  ( $v=0$ ) and  $b^1\Sigma_g^+$  ( $v=0$ ). The experimental errors in the cross sections are about 35%.

tion for the exchange amplitude. However, the total cross section near 8 eV calculated by these authors is only about a factor of 2 less than the experimental value.

The magnitude and energy dependence of the differential vibrational cross sections observed in the 4–15-eV range lead us to interpret the results in terms of resonances. A comprehensive angular-dependence measurement is necessary to identify directly the symmetries of the excited  $O_2^-$  states involved. Nevertheless, it is possible to make some inferences based on the present results and the current information on the  $O_2^-$  states.

There are 46 negative-ion states, arising from the interaction between the  $O^-(^2P)$  state and the  $^3P$ ,  $^1D$ , and  $^1S$  states of atomic oxygen; but for the present purpose we should consider only those  $O_2^-$  states which intercept the Franck-Condon region within the 6–11-eV range and which are not restricted by the selection rules governing the attachment process.<sup>11</sup> *A priori* calculations of the potential-energy curves<sup>12,13</sup> of  $O_2^-$  show that the only states which meet these criteria are the  $^2\Pi_u$  and  $^4\Sigma_u^-$  states. The  $^2\Sigma_g^+$  state of  $O_2^-$  also lies at low energies, but it is not accessible for attaching an electron to the target  $X^3\Sigma_g^-$  state because this requires a change in reflection symmetry ( $- \rightarrow +$ ) during the attachment process.

The potential-energy curve of the  $^2\Pi_u$  state in the Franck-Condon region has also been obtained by O'Malley<sup>14</sup> by fitting empirically to the dis-

sociative attachment cross section in hot  $O_2$ . Decay of the  $^2\Pi_u$  state to any  $O_2$  state lying energetically below the  $^2\Pi_u$  state should lead to a peak in the cross section near 7.8 eV. Since the peaks in the vibrational cross sections of Fig. 2 occur at higher energies, it is improbable that the  $^2\Pi_u$  state makes the dominant contribution to these cross sections.

We conclude that the  $^4\Sigma_u^-$  state is predominantly responsible for the vibrational excitation peak near 9.5 eV. This is not unexpected since the  $^4\Sigma_u^-$  is one of two shape resonances<sup>12</sup> (another one is the  $^2\Sigma_u^-$  state) which are formed by adding a  $2p\sigma_u$  electron to the ground  $X^3\Sigma_g^-$  state of  $O_2$ . Decay of shape resonances into their own parents is always favorable.<sup>3</sup> The dominant scattering partial wave for both resonant states is expected to be  $p\sigma$ .

The peaks in the electronic excitation cannot be explained by invoking the  $^4\Sigma_u^-$  state, since quartet states cannot decay into either of the singlet excited states. The excitation of the  $a^1\Delta_g$  state probably proceeds predominantly via the  $^2\Pi_u$  resonance as discussed by Burrow,<sup>15</sup> and the excitation mechanism of the  $b^1\Sigma_g^+$  state is still uncertain.

We wish to thank P. D. Burrow and A. Herzenberg for helpful discussions on many aspects of the present work. We also thank J. Kearney for technical assistance.

\*Research sponsored by the U.S. Army Research Office and the Defense Nuclear Agency under Subtask HD010, Work Unit 40, "Laboratory reaction rate studies."

<sup>1</sup>H. S. W. Massey, *Electronic and Ionic Impact Phenomena* (Oxford Univ. Press, Oxford, England, 1969), Vol. 2, Chap. 11.

<sup>2</sup>G. Herzberg, *Spectra of Diatomic Molecules* (Van Nostrand, Princeton, N.J., 1967), Chap. VI.

<sup>3</sup>For a review of resonances in diatomic molecules see G. J. Schulz, *Rev. Mod. Phys.* **45**, 423 (1973).

<sup>4</sup>Z. Pavlovic, M. J. W. Boness, A. Herzenberg, and G. J. Schulz, *Phys. Rev. A* **6**, 676 (1972).

<sup>5</sup>J. Comer and F. H. Read, *J. Phys. B: Proc. Phys. Soc., London* **4**, 1055 (1971).

<sup>6</sup>L. Sanche and G. J. Schulz, *Phys. Rev. A* **5**, 1672 (1972).

<sup>7</sup>R. W. LaBahn and J. Callaway, *Phys. Rev. A* **2**, 366 (1970).

<sup>8</sup>S. Trajmar, D. C. Cartwright, and W. Williams, *Phys. Rev. A* **4**, 1482 (1971).

<sup>9</sup>L. Sanche and G. J. Schulz, *Phys. Rev. A* **6**, 69 (1972).

<sup>10</sup>P. S. Julienne and M. Krauss, *J. Res. Nat. Bur. Stand., Sect. A* **76**, 661 (1972).

<sup>11</sup>G. H. Dunn, *Phys. Rev. Lett.* **8**, 62 (1962).

<sup>12</sup>M. Krauss, D. Neumann, A. C. Wahl, G. Das, and W. Zemke, *Phys. Rev. A* **7**, 69 (1973).

<sup>13</sup>H. H. Michels and F. E. Harris, in *Proceedings of the Seventh International Conference on the Physics of Electronic and Atomic Collisions, Amsterdam, 26-30*

*July 1971. Invited Talks and Progress Reports*, edited by T. R. Govers and F. J. de Herr (North-Holland, Amsterdam, 1972), p. 1170.

<sup>14</sup>T. F. O'Malley, *Phys. Rev.* **155**, 59 (1967).

<sup>15</sup>P. D. Burrow, to be published.

## X-Ray to Visible Wavelength Ratios

Richard D. Deslattes and Albert Henins

*National Bureau of Standards, Washington, D.C. 20234*

(Received 14 August 1973)

The lattice repeat distance of a nearly perfect single crystal of silicon has been measured in terms of the visible wavelength of a stabilized He-Ne laser. This crystal subsequently has been used to diffract reference x-ray lines (Cu  $K\alpha_1$ , Mo  $K\alpha_1$ ) thereby establishing their wavelength relative to visible standards. In terms of the x-ray scale in which  $\lambda(\text{Cu } K\alpha_1) = 1.537400 \text{ kxu}$ , the conversion factor is  $\Lambda_{\text{Cu}} = 1.0020802 \text{ \AA/kxu}$  (1 ppm); if  $\lambda(\text{Mo } K\alpha_1) = 0.707831 \text{ kxu}$ ,  $\Lambda_{\text{Mo}} = 1.0021017 \text{ \AA/kxu}$  (0.6 ppm).

We have measured the wavelengths of two x-ray reference lines, Cu  $K\alpha_1$  and Mo  $K\alpha_1$ , in terms of the 633-nm wavelength of a  $^3\text{He-}^{20}\text{Ne}$  laser stabilized with respect to its Lamb dip. The x-ray measurements were carried out in two steps: In the first of these, we measured the spatial periodicity of a silicon single crystal by means of simultaneous x-ray and optical interferometry of displacements along the (110) crystallographic direction. In the second, we used a closely related sample of this material to diffract Cu  $K\alpha_1$  and Mo  $K\alpha_1$  x-radiation and obtained the wavelengths via double-crystal spectrometry. This work is a part of a larger measurement program which has been outlined previously<sup>1</sup> and is the first report of results at or exceeding the targeted accuracy.

The principle of the combined x-ray and optical interferometer used to obtain the results reported here is illustrated in Fig. 1. The standing x-ray wave field produced by the two crystals belonging to the stationary assembly, *a*, is intercepted by the third crystal which is part of the movable assembly, *b*. Such a symmetric, Laue-case interferometer produces cosine fringes observed at the x-ray detector, *c*, with translation along the crystal diffraction vector as suggested by the large arrow.<sup>2</sup> The optical cavity indicated has one mirror attached to the stationary assembly and one to the moving assembly. It is a high-finesse Fabry-Perot interferometer whose resonant transmission maxima are detected by the photomultiplier indicated at *d*.

The silicon crystal from which the x-ray inter-

ferometer was made was dislocation-free, vacuum float-zoned material.<sup>3</sup> The optical cavity was hemispherical and operated with a mean order number of  $10^3$  and a working finesse of  $10^3$  or more. The curved mirror radius was 120 cm so that the Fresnel phase shift,<sup>4</sup> viz.,  $\pi^{-1} \cos^{-1}[(1 - L/R)^{1/2}]$ , gave a correction of 2.50 ppm near midrange. For measurements made over the entire range,  $0.8 \times 10^3 \lambda/2 < L < 1.4 \times 10^3 \lambda/2$ , this correction would have varied from 2.8 to 2.2 ppm had use been made of the whole range. Laser output was mode matched into the optical cavity by a single lens.<sup>4</sup> Decoupling of the laser from the cavity was effected by a quarter-wave-plate,

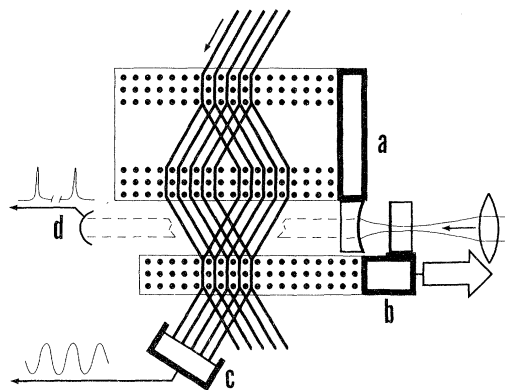


FIG. 1. Principle of simultaneous x-ray and optical interferometry of a common base line. Stationary and moving parts are labeled *a* and *b*, respectively. The x-ray detector is *c* and the optical detector is *d*.